Structural origin of dynamic heterogeneity in three-dimensional colloidal glass formers and its link to crystal nucleation

2010 J. Phys.: Condens. Matter 22 232102

(http://iopscience.iop.org/0953-8984/22/23/232102)

IOP FTC
IOP Publishing
Journal of Physics: Condensed Matter
J. Phys.: Condens. Matter **22** (2010) 232102 (10pp)
doi:10.1088/0953-8984/22/23/232102

FAST TRACK COMMUNICATION

Structural origin of dynamic heterogeneity in three-dimensional colloidal glass formers and its link to crystal nucleation

Takeshi Kawasaki and Hajime Tanaka

Institute of Industrial Science, University of Tokyo, 4-6-1 Komaba, Meguro-ku, Tokyo 153-8505, Japan

E-mail: tanaka@iis.u-tokyo.ac.jp

Received 2 April 2010, in final form 30 April 2010
Published 21 May 2010
Online at stacks.iop.org/JPhysCM/22/232102

Abstract
The physical understanding of glass transition remains a major challenge of physics and materials science. Among various glass-forming liquids, a colloidal liquid interacting with hard-core repulsion is now regarded as one of the most ideal model systems. Here we study the structure and dynamics of three-dimensional polydisperse colloidal liquids by Brownian dynamics simulations. We reveal that medium-range crystalline bond orientational order of the hexagonal close packed structure grows in size and lifetime with increasing packing fraction. We show that dynamic heterogeneity may be a direct consequence of this transient structural ordering, which suggests its origin is thermodynamic rather than kinetic. We also reveal that nucleation of crystals preferentially occurs in regions of high medium-range order, reflecting the low crystal–liquid interfacial energy there. These findings may shed new light not only on the fundamental nature of the glass transition, but also the mechanism of crystal nucleation.

S Online supplementary data available from stacks.iop.org/JPhysCM/22/232102/mmedia

(Some figures in this article are in colour only in the electronic version)

1. Introduction

One of the most puzzling features of glass transition is the dramatic dynamical slowing down towards the glass-transition point while accompanying no noticeable change in the static structure [1–6]. It was revealed that supercooled liquids exhibit spatially heterogeneous dynamics [2–5, 7] and their characteristic lengthscale measured by dynamic quantities increases towards the glass-transition point [8–16]. This dynamic heterogeneity is regarded as a key feature of a supercooled liquid state. Furthermore, a link between local dynamics and local structure was suggested for spin glasses [17, 18] and also for 2D [8] and 3D supercooled liquids [19–21]. However, the answers to fundamental questions, such as whether such a growing dynamical correlation is a cause of slow dynamics or merely its manifestation and whether the origin of dynamic heterogeneity is static or dynamical have remained elusive.

To address these issues, a hard-sphere system may be quite useful because of its simple interaction. We stress that a hard-sphere system is often used as the most ideal model system for studying phase transitions observed in condensed matter [22]. The control parameter of this system is the volume fraction ϕ rather than the temperature T, and the effective temperature is $T_{\rm eff} = 1/\phi$. Colloidal suspensions and granular materials are typical examples of realistic hard-sphere systems. Glass transition in a colloidal suspension was first observed by Pusey and van Megen about two decades ago [22]. Later, it was observed by light-scattering experiments (see, e.g., [23]) that polydisperse colloidal suspensions exhibit a two-step relaxation where fast β relaxation is followed by a slow α relaxation and the structural (α) relaxation time τ_α dramatically increases when approaching the glass-transition volume fraction $\phi_{\rm g}$, but without a noticeable structural change. Recently, confocal microscopy has allowed simultaneous access to the structure and dynamics at a single-

particle level, which leads to direct detection of dynamic heterogeneity [14, 15]: heterogeneous particles' trajectory patterns, direct visualization of dynamic heterogeneity on a particle level, and the growth of the dynamical coherence length characterized by the mobility of particles towards ϕ_g. Using dynamic light scattering, Berthier *et al* obtained the multi-point dynamic susceptibilities and showed evidence of the growing lengthscale towards ϕ_g [16].

A hard-sphere system also makes a theoretical treatment simple. For example, the validity of mode-coupling theory (MCT) [24] has been intensively checked in colloidal liquids [6]: for example, a power-law divergence of τ_α towards mode-coupling ϕ_c, $\tau_\alpha \propto (\phi_c - \phi)^{-\gamma}$, has been confirmed and ϕ_c beyond which the system becomes nonergodic was estimated as $\phi_c \approx 0.58$ [6, 23]. However, recent experimental and numerical studies [25] revealed that even above ϕ_c, a colloidal suspension with the size polydispersity $\Delta \cong 10\%$ still remains ergodic and exhibits slow structural relaxation. As in ordinary glass-forming liquids, τ_α is well described by the Vogel–Fulcher–Tammann (VFT)-like law, $\tau_\alpha \propto \exp[D\phi/(\phi_0 - \phi)^\delta]$ with $\delta = 2$ and the ideal glass-transition point $\phi_0 = 0.637$, which is slightly below the random close packing (rcp) fraction ϕ_{rcp}. Here D is the fragility index [2], which is larger for a less fragile liquid. To understand such a crossover from a MCT regime to a regime of activated dynamics, the cooperative particle motion (dynamic heterogeneity) is thought to be very important [16]. However, there is no consensus on its physical origin so far.

Following pioneering works in the early days [8, 17–21], there was further evidence that dynamic heterogeneity has a link to a static structure of a supercooled liquid [26–36], although the possibility of a purely kinetic origin was also suggested (e.g., [37]). Recent works seeking a static origin of dynamic heterogeneity focused on icosahedral order [21, 34, 35], amorphous order [33], inherent structure [30, 38, 39], defect density [32], or crystal-like bond orientational order [27–29]. Here we summarize our recent studies, which are the basis of the present work. In a two-dimensional (2D) repulsive polydisperse colloidal system [28], we found that medium-range crystalline bond orientational order (MRCO) emerges in a supercooled liquid and its size and lifetime increases towards ϕ_g. It was shown that particles belonging to MRCO are slower than the other particles, indicating that dynamic heterogeneity is a consequence of MRCO. A similar behaviour is also seen in two different 2D systems, a driven polydisperse granular liquid [29] and a spin liquid with energetic frustration [27]. A local structural ordering has also been reported for a bidisperse colloidal glass in a supercooled state [31] and during ageing [36]. In colloidal and granular liquids, crystallization is prevented by polydispersity, whereas in spin liquids it is by energetic frustration. Despite this difference in the origin of frustration against crystallization, the basic behaviour is strikingly similar between them, indicating some universality.

In these 2D systems, we can easily access structural information. At the same time, the ordering of 2D hard disks is known to be peculiar and more importantly 2D systems have a rather weak link to real glass-forming liquids. Another important issue is whether the hexatic order found in 2D systems is a manifestation of crystal-like order [28, 40] or icosahedral order [34, 41]. This question is linked to the fundamental origin of frustration, which leads to glass formation [40]. So we study the structural origin of dynamic heterogeneity in 3D polydisperse colloidal systems (hard-sphere-like particles interacting with the Weeks–Chandler–Andersen (WCA) repulsive potential [42]) using Brownian dynamics simulations (see supplementary data, available at stacks.iop.org/JPhysCM/22/232102/mmedia for the details). In this model, the glass-forming ability can continuously be controlled by changing the degree of polydispersity [28, 43]: the higher the polydispersity, the higher the nucleation barrier [44]. Experimentally, polydisperse colloidal dispersions have often been used as a model glass-forming liquid and the important roles of polydispersity in the glass-forming ability has recently been emphasized [14, 15, 25, 44–48]. In this communication, we also study how transient structural ordering in a supercooled state affects the nucleation of crystals.

2. Results and discussion

First we describe the phase behaviour of this system as a function of Δ and ϕ [49, 50]. A system of small polydispersity ($\Delta < 6\%$) easily crystallizes when we increase the volume fraction ϕ above the freezing point. A system of larger Δ ($\geqslant 7\%$) [51] is vitrified without crystallization in our simulations. As a very rare event, however, we observe crystal nucleation for $\Delta = 6\%$ (see below). Whether a system crystallizes or vitrifies is also checked by the ϕ-dependence of the potential energy of a system, $\langle U \rangle = \langle \sum_{k<j} U_{jk} \rangle$ (see figure 1(a)). We observe a step-like behaviour which is characteristic of a first-order liquid–crystal transition. In figure 1(b), we show the radial distribution function, $g(r)$. For a monodisperse system, we confirm the occurrence of a liquid–crystal transition, which accompanies a sudden development of long-range positional order and the resulting density change. For a larger polydispersity $\Delta > 6\%$, on the other hand, such a drastic structural change is not seen up to a higher ϕ where the system becomes nonergodic: crystallization is avoided and a system eventually vitrifies for $\phi \geqslant \phi_g$. It is worth noting that even for $\Delta \geqslant 6\%$, a second peak of $g(r)$ shows splitting at high ϕ (see figure 1(b)), indicating the development of some structural order in a supercooled liquid [14, 28, 29, 52]. These features are common for $\Delta = 12$ and 18%, although less significant (not shown). Such structural ordering can also be seen in the structure factor $S(q)$ (q: wavenumber) in figure S1 (available at stacks.iop.org/JPhysCM/22/232102/mmedia). Here it may be worth noting that similar local structural ordering has also been observed in experiments of a 2D magnetic colloidal system [53].

Next we show dynamics in the glass-forming Δ region. Figure 1(c) shows the self-part of the intermediate scattering function (ISF), $F(q_p, t)$, for $\Delta = 6\%$. The structural (α) relaxation slows down and is more stretched with an increase in ϕ. The long-time decay of the ISF is fitted by a two-step relaxation: $F(q_p, t) = (1 - A)\exp[-(t/\tau_\beta)] +$

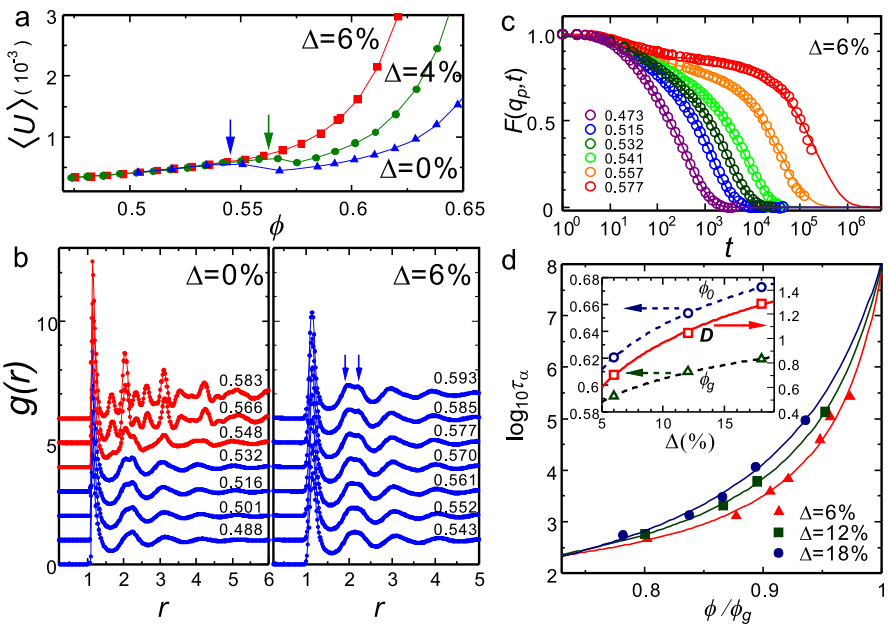

Figure 1. Roles of the polydispersity in the phase behaviour and dynamics. (a) ϕ-dependence of the potential energy $\langle U \rangle$ for $\Delta = 0\%$, 4% and 6%. There are non-monotonic changes in the curves for $\Delta = 0$ and 4%, which are indicated by the arrows. They are signatures of disorder–order transition, i.e., crystallization. (b) ϕ-dependence of the radial distribution function $g(r)$ for $\Delta = 0\%$ and $\Delta = 6\%$. The blue colour means disordered, whereas the red colour means ordered. Comparison of (a) with (b) tells us that there is no disorder–order transition for $\Delta = 6\%$. However, we can see the splitting of the second peak at high ϕ even for $\Delta = 6\%$ (see the arrows), indicating the possible existence of medium-range order. (c) ϕ-dependence of $F(q_p, t)$ for $\Delta = 6\%$. The solid lines indicate the fitting functions (KWW functions). (d) The dependence of τ_α on ϕ/ϕ_g for $\Delta = 6$, 12 and 18%. The solid lines are the results of the VFT fitting. The inset shows the Δ-dependence of ϕ_0, ϕ_g and D. The lines are eye guides.

$A \exp[-(t/\tau_\alpha)^\beta]$, where A is the Debye–Waller (DW) factor, τ_β is the fast β relaxation time, τ_α is the α relaxation time and β is the Kohlrausch–Williams–Watts (KWW) stretching parameter. Since in a hard-sphere system $1/\phi$ plays the same role as the temperature in usual liquids, τ_α is well fitted by the VFT function for ϕ: $\tau_\alpha = \tau_0 \exp[D\phi/(\phi_0 - \phi)]$. We note that the larger fragility index D means less fragile [2]. The ϕ-dependencies of A and β for $\Delta = 6\%$ are shown in figure S2 (available at stacks.iop.org/JPhysCM/22/232102/mmedia).

Figure 1(d) shows the ϕ/ϕ_g-dependence of τ_α (Angell plot [2]) obtained from the above fittings for $\Delta = 6\%$, 12% and 18%. We define ϕ_g as ϕ where $\tau_\alpha = 10^8$. At a low Δ, τ_α steeply increases with increasing ϕ or ϕ/ϕ_g, which is characteristic of a fragile glass former. For a large Δ, on the other hand, it behaves more Arrhenius-like. The inset of figure 1(d) shows the Δ dependence of ϕ_0, ϕ_g and D, indicating that ϕ_0, ϕ_g and D all increase with Δ (see also table S1, available at stacks.iop.org/JPhysCM/22/232102/mmedia). This suggests that a system with larger Δ, which suffers from stronger frustration against crystallization, is less fragile. We stress that the polydispersity Δ, which controls the degree of frustration against crystallization, governs not only glass-forming ability, but also the fragility, or the glass-transition behaviour [27–29, 40]. In relation to this, it is worth mentioning that the fragility of a colloidal liquid can also be controlled by the softness of particles [54]. We speculate that softness of particles may lead to larger structural fluctuations, which suppress crystallization.

Next we focus on the correlation between structure and dynamics. Figure 2(a) shows a snapshot of a liquid structure for $\phi = 0.577$ at $\Delta = 6\%$. The particle colour represents the value of bond orientational order (BOO) parameter $\bar{Q}_6^k$ [55–57]. We can clearly see the spatial heterogeneity of the distribution of the order parameter $\bar{Q}_6^k$ (see supplementary data, available at stacks.iop.org/JPhysCM/22/232102/mmedia for the definition). Figure 2(b) shows a snapshot of highly ordered particles with $\bar{Q}_6^k > 0.25$. We confirm that the lifetime of clusters of highly ordered particles is longer than the structural relaxation time τ_α. We emphasize that these clusters are spatio-temporally fluctuating in a supercooled liquid and do not grow with time and thus they are 'not' nuclei of phase-separated crystals. Next, to elucidate a structural feature of the clusters, we show $g(r)$ of particles belonging to the clusters (see figure 2(c)) together with $g(r)$ of a crystal observed at $\phi = 0.577$ and $\Delta = 0\%$. $g(r)$ of clusters have peaks (and shoulders) characteristic of the crystal. We also calculate the bond angle distribution $f(\theta_j^{kl})$ (figure 2(d)) of particles belonging to clusters shown in figure 2(b) and that for the crystal. Here θ_j^{kl} is the angle between bonds connecting particle j to its nearest neighbour particles k and l, which is calculated as $\theta_j^{kl} = \cos^{-1}(\vec{r}_{jk} \cdot \vec{r}_{jl}/|\vec{r}_{jk}||\vec{r}_{jl}|)$. The peak positions of $f(\theta_j^{kl})$ for clusters are 60°, 90°, 120° and 180°. This indicates that particles in clusters have the same BOO as the crystal. Thus we call these slow clusters as medium-range crystalline order (MRCO), as in 2D systems [27–29]. However, it should be noted that there is no density change associated with MRCO, which can be seen from the absence

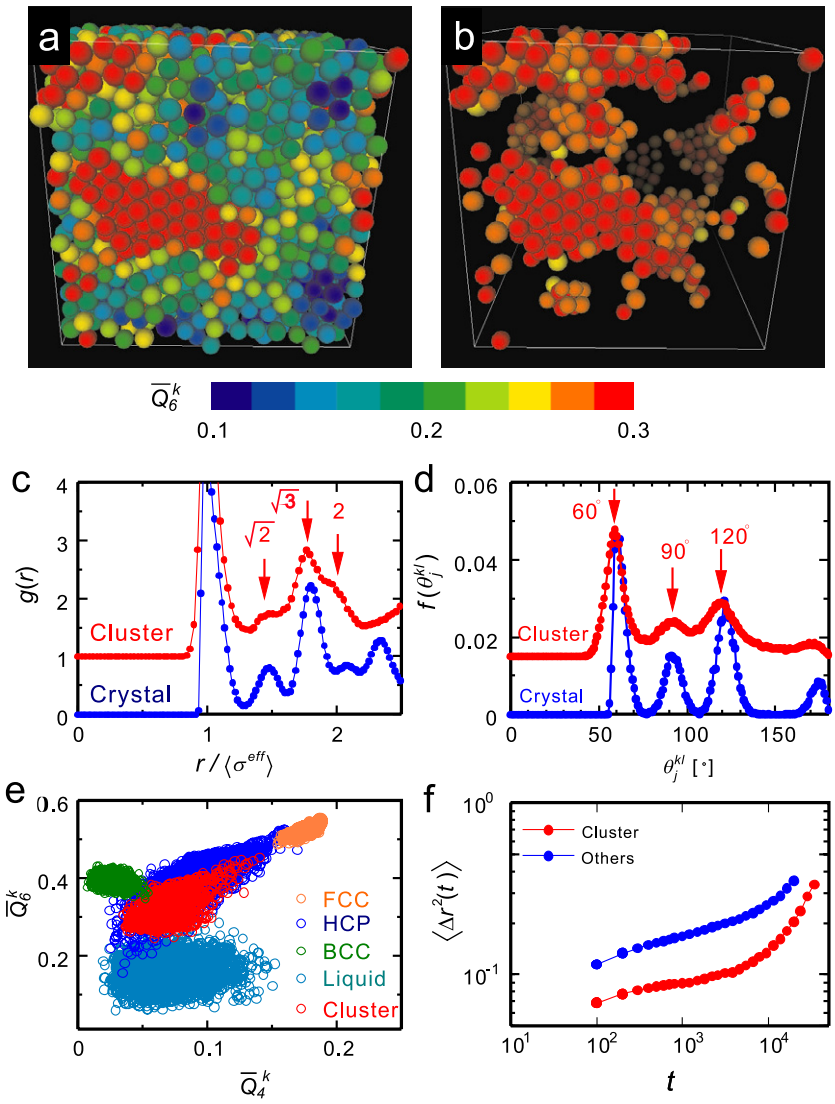

Figure 2. Structural features of slow particle clusters. (a) Snapshot of a liquid structure for $\phi = 0.577$ and $\Delta = 6\%$. The particle colour represents the value of $\bar{Q}_6^k$ (see the colour bar). (b) Snapshot of clusters of highly ordered particles with $\bar{Q}_6^k > 0.25$ in (a). (c) Radial distribution functions of particles belonging to the clusters in (b) and an fcc crystal observed at $\phi = 0.577$ for $\Delta = 0$. (d) The bond angle distribution $f(\theta_j^{kl})$ of the particles belonging to the clusters in (b) and the fcc crystal observed at $\phi = 0.577$ for $\Delta = 0$. (e) Correlation map of the two bond orientational order parameters, $\bar{Q}_4^k$ and $\bar{Q}_6^k$, for fcc, hcp and bcc crystals ($\phi = 0.577$, $\Delta = 0$), a disordered liquid ($\phi = 0.421$, $\Delta = 6\%$) and the clusters in (b). (f) The mean square displacements $\langle\Delta r^2(t)\rangle$ of particles belonging to the clusters in (b) and the other particles in (a). The solid lines are guides to the eye.

of excess scattering in the low q region in $S(q)$ (see the curve of $(t - t')/\tau_\alpha < 0$ in figure 4(c)). This indicates that MRCO possesses BOO, but no translational order. For further characterization of the cluster structure, we make a correlation map of the two types of BOO parameters, $\bar{Q}_4^k$ and $\bar{Q}_6^k$, [57, 58] for the clusters in figure 2(b), crystals (fcc, hcp and bcc), and a disordered liquid, in figure 2(e). The results clearly tells us that the BOO parameters' distribution for the clusters is very similar to that for hcp, but very different from those of the other structures (fcc and bcc).

In particular, our results rule out a possibility that MRCO has an icosahedral order. This has an important implication on the meaning of hexatic order in a 2D hard-sphere-like system [28, 34]. First, $g(r)$ of the clusters has peaks or shoulders around 1.0, 1.4, 1.7, and 2.0, which correspond to those of the crystal's $g(r)$ (see figure 2(c)). For an icosahedral structure, such peaks should be observed at 1.05, 1.70, and 2.0 [59]. Thus, the presence of a distinct peak at 1.4 (figure 2(c)) indicates that the clusters do not have icosahedral order. Second, the bond angle distribution $f(\theta)$ in figure 2(d) shows that $f(\theta)$ of the clusters has peaks at 60°, 90°, 120°, and 180°. On the other hand, for an icosahedral structure $f(\theta)$ should have peaks at 60°, 108°, ... [41]. The presence of a peak at 90° also rules out the possibility of icosahedral order in the clusters. Finally, a correlation map of Q_4 and Q_6 also supports that the clusters have a hcp-like bond orientational order. The non-averaged values of Q_4 and Q_6 for an ideal icosahedral structure are known to be 0 and 0.663, respectively [56], which also suggests that clusters do not have icosahedral order. All these indicate that

the clusters have hcp-like bond orientational order and do not possess icosahedral order. For hard-sphere systems, thus, we conclude that a supercooled liquid has little tendency to form icosahedral order, but instead has a tendency to form hcp-like bond orientational order. It may be worth noting that there is no clear reason to expect icosahedral order for a hard-sphere system. We note, however, that we cannot rule out the presence of a small amount of short-lived transient icosahedral structures in a liquid.

The reason why a system favours hcp-like and not fcc-like bond orientational order in the supercooled state is an interesting question. The most stable structure for a system of no frustration ($\Delta = 0\%$) is known to be an fcc crystalline structure. First of all, positional order is easily destroyed by the introduction of weak frustration (see figure 1). Even under frustration, bond orientational order still survives. Our results indicate that hcp-like bond orientational order is more favourable than fcc-like, because the former allows more fluctuations in the structure (or, structural entropy), which can be seen in the correlation map between Q_4 and Q_6: the distribution of bond orientational orders is much broader for hcp than fcc and bcc. This may also be related to the softer nature of hcp than for fcc against some deformation modes [60], although our cluster with hcp-like bond orientational order is not a crystal. In relation to this, it may be worth noting that as a very rare event, we happen to observe crystal nucleation in a sample of $\Delta = 6\%$. In this case, a crystal with more fcc-like bond orientational order is nucleated from in a region of high MRCO with hcp-like bond orientational order. This suggests that the energy barrier for nucleation of a crystal is lower in a region of higher MRCO that in that of lower MRCO, as will be shown below.

Now we focus on the dynamics of particles belonging to MRCO. Figure 2(f) compares the mean square displacement $\langle \Delta r^2(t) \rangle$ of particles belonging to MRCO with that of the other particles. This indicates that particles belonging to MRCO are much slower than the other particles and dynamic heterogeneity is closely linked to MRCO. We also find that there is a distinct negative correlation between the particle mobility and the DW factor (solidity): slower particles have higher DW factors. Note that the DW factor, A, characterizes the contribution of the slow structural relaxation with respect to the total relaxation (see figure 1(c)). This is not only consistent with what was reported by Widmer-Cooper and Harrowell [26], i.e., the relationship between the short-time fluctuations (fast β process) and long-time dynamic propensity (α process), but also provides a further link between the DW factor and the degree of structural order, i.e., MRCO. Thus, we establish the relationship between the DW factor (solidity), long-time mobility, and MRCO. This leads to a scenario [61] that the presence of MRCO may be an origin of dynamic heterogeneity in a supercooled liquid for both 2D [27–29] and 3D systems.

Dynamic heterogeneity is often characterized by a four-point density correlator [12] (see supplementary data, available at stacks.iop.org/JPhysCM/22/232102/mmedia). Figure 3(a) shows the ϕ-dependence of the dynamic susceptibility $\chi_4(t)$. To extract the dynamical correlation length ξ_4, we fit the following Ornstein–Zernike function to $S_4(\vec{q}, \tau_{\rm H})$ (see supplementary data, available at stacks.iop.org/JPhysCM/22/232102/mmedia) as $S_4(\vec{q}, \tau_{\rm H}) = S_0/[1 + (\xi_4 q)^2]$ (see figure 3(b)). Figure 3(c) shows the ϕ-dependence of the dynamical correlation length ξ_4 and the characteristic size of MRCO ξ (see supplementary data, available at stacks.iop.org/JPhysCM/22/232102/mmedia) for $\Delta = 6$, 12 and 18%. The ϕ-dependence of $\xi_{(4)}$ is well fitted by the following power law (solid lines in figure 3(c)): $\xi_{(4)} = \xi_{(4)0}[(\phi^{-1} - {\phi_0}^{-1})/{\phi_0}^{-1}]^{-2/d}$, where d is the spatial dimensionality ($d = 3$). We note this exponent $2/d$ is consistent with the Ising criticality [61]. Here ϕ_0 is independently determined by the VFT fitting for τ_α (figure 1(d)) and thus ξ_{40} is the only adjustable parameter. The values of ϕ_0 and $\xi_{(4)0}$ are available in the caption of figure 3(c). We note that the correlation length of the BOO, ξ_6, also behaves as ξ and ξ_4 (see figure S3, available at stacks.iop.org/JPhysCM/22/232102/mmedia). The strikingly similar behaviour of ξ and ξ_4 further supports a link between structure and dynamics.

Next we consider the relationship between $\xi_{(4)}$ and τ_α (see figure 3(d)). We find the relation $\tau_\alpha = \tau_0 \exp[D\phi/(\phi_0 - \phi)] = \tau_0 \exp[D(\xi_{(4)}/\xi_{(4)0})^{d/2}](d = 3)$, although we cannot completely exclude other functional forms, e.g., a power law. This link between $\xi_{(4)}$ and τ_α suggests that the growth of MRCO may be an origin of dynamical slowing down towards $\phi_{\rm g}$. The exponent $d/2$ is apparently consistent with the scaling argument based on the random first-order transition theory [40, 62, 63], but we note that our MRCO is distinctly different from 'amorphous order' assumed there. We also show the relationship between the two-body translational correlation contribution to the excess entropy s_2 and ξ/ξ_0 (figure 3(e)). This excess entropy is given by $s_2 = -(\phi/2)\int d\vec{r}\,[g(\vec{r})\ln g(\vec{r}) - g(\vec{r}) + 1]$ [64, 65]. s_2 decreases with an increase in $\xi_{(4)}/\xi_{(4)0}$. We find that s_2 almost linearly decreases as a function of $(\xi_{(4)}/\xi_{(4)0})^{d/2}$ (see solid lines in figure 3(e)). The same relation has been seen for 2D systems with $d = 2$ [28, 29], implying the generality of the relation. This suggests that the decrease of the structural entropy is induced by structural ordering.

The above results suggest the power-law divergence of the static correlation length towards ϕ_0. This is suggestive of a thermodynamic singularity at ϕ_0. However, it is not clear at this moment whether the correlation length really diverges or not. This originates from the intrinsic inaccessibility to the ideal glass-transition point because of the extremely steep slowing down towards it. A decoupling between ξ and ξ_4 was also recently suggested for a 2D liquid on a curved surface [35]. In relation to this, it was proposed that there is no singularity above $T = 0$ K [32, 66, 67]. This problem may be viewed as whether the ordering transition is second-order, rounded, or weakly first-order. We speculate that even the dynamic order–disorder transition scenario proposed in [37], which apparently does not involve any thermodynamic singularity, might have a connection to our static transition scenario via 'hidden' structural ordering. Since the ideal glass-transition point is intrinsically an unattainable critical point, as stated above, further careful studies are necessary on these points.

Finally, we describe a novel kinetic pathway of crystal nucleation found in a system of $\Delta = 6\%$. Crystal nucleation

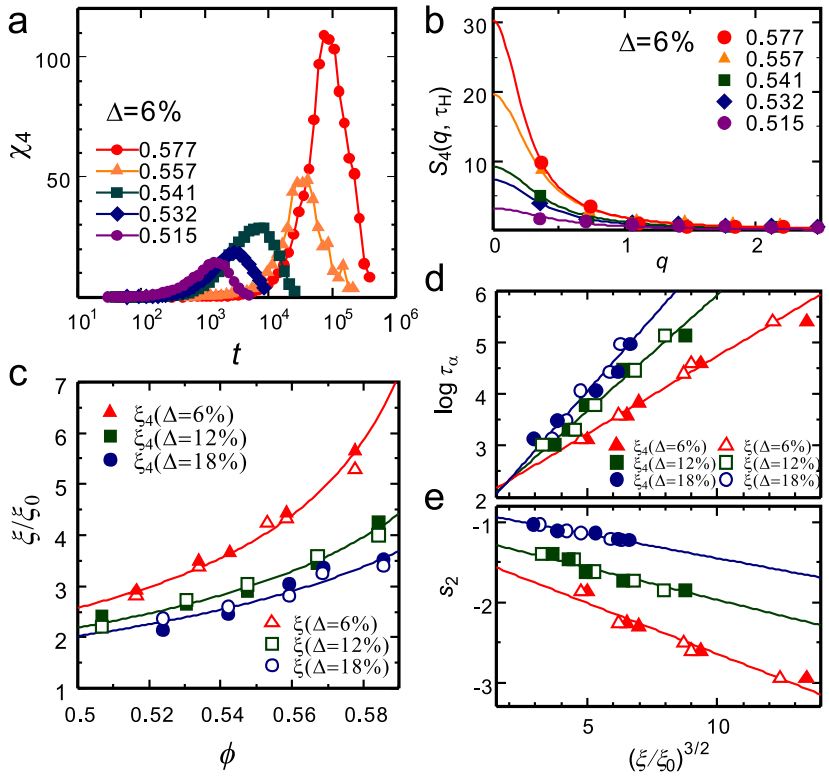

Figure 3. Relationship between structure and dynamics. (a) ϕ-dependence of $\chi_4(t)$ for $\Delta = 6\%$. We define the time of the peak as $t = \tau_{\mathrm{H}}$. (b) ϕ-dependence of $S_4(q, \tau_{\mathrm{H}})$ for $\Delta = 6\%$. The solid lines indicate the Ornstein–Zernike function $S_0/[1 + (\xi_4 q)^2]$. From the fitting, we obtain the dynamic correlation length ξ_4. (c) ϕ-dependence of ξ and ξ_4 for $\Delta = 6$, 12 and 18%. The lines are fittings by $\xi_{(4)} = \xi_{(4)0}[(\phi^{-1} - \phi_0)^{-1}/\phi_0{}^{-1}]^{-2/3}$. The bare correlation length ξ_0 for various Δ's are obtained as $\xi_0(\Delta = 6\%) = 0.72$, $\xi_0(\Delta = 12\%) = 0.70$ and $\xi_0(\Delta = 18\%) = 0.51$ with $\bar{Q}_{60}(\Delta = 6\%) = 0.27$, $\bar{Q}_{60}(\Delta = 12\%) = 0.23$ and $\bar{Q}_{60}(\Delta = 18\%) = 0.23$. The bare correlation length ξ_{40} for various Δ's are obtained as $\xi_{40}(\Delta = 6\%) = 0.69$, $\xi_{40}(\Delta = 12\%) = 0.68$ and $\xi_{40}(\Delta = 12\%) = 0.65$. (d) Relation between τ_α and $(\xi/\xi_0)^{3/2}$ for $\Delta = 6$, 12 and 18%. The solid line is a fitting by $\tau_\alpha = \tau_0 \exp[D(\xi/\xi_0)^{3/2}]$. (e) Relation between s_2 and $(\xi/\xi_0)^{3/2}$ for $\Delta = 6$, 12 and 18%. The dashed lines are $s_2 = C_0(\xi/\xi_0)^{3/2} + C_1$. C_0 and C_1 are adjustable parameters.

is an intrinsic kinetic pathway towards an equilibrium state from a metastable supercooled liquid, which is suggestive of a deep link between vitrification and crystallization [27, 40]. Recently, an important relationship between glass formation, dynamic heterogeneity and the resulting breakdown of the Stokes–Einstein relation, and crystal nucleation has been reported for a model network-forming liquid [68] by molecular-dynamics simulations. Furthermore, the interplay between dynamics and crystallization has been studied for both monodisperse and polydisperse colloidal systems [69]. Here we describe a novel kinetic pathway of crystal nucleation found in a hard-sphere-like system of $\Delta = 6\%$. Although the probability is very low, crystallization takes place for $\Delta = 6\%$ as a rare event. For $\Delta = 12$ and 18%, on the other hand, we never see any indication of such crystallization in our simulation time, in accord with experiments [25, 46, 47]: the frustration is strong enough to kinetically avoid crystallization. We note that crystallization must involve fractionation of particles above $\Delta > 6$ % [49].

Figure 4(a) shows the birth process of a crystal. Interestingly, a crystal with fcc + hcp BOO (coloured green), suggestive of a random hexagonal close packing (rhcp) structure [44], is nucleated inside a region of high MRCO with hcp-like BOO (coloured red), We can also see the transition from MRCO to a crystal in the Q_4–Q_6 mapping in figure 4(b). We emphasize that before crystallization the structure factor $S(q)$ of a supercooled liquid does not have any excess scattering around a wavenumber corresponding to the size of MRCO, ξ, but crystallization induces a steep rise at low q, reflecting a higher density of crystal than a liquid (see figure 4(c)). We can use (i) decoupling of MRCO and coupling of a crystal nucleus with density change (figure 4(c)) and (ii) the local symmetry (BOO) (figure 4(b)) as fingerprints for judging whether crystal nucleation takes place or not. Figure 4(d) shows the temporal evolution of the number of particles belonging to the crystal nucleus, N_{crystal}, as well as the scattering intensity at the lowest q, $S(q_{\mathrm{min}})$. These results indicate the growth of the nucleus of the crystal, which has a higher density than the surrounding liquid.

This finding may have significant implications on the very nature of MRCO and crystal nucleation in a supercooled liquid. A supercooled state of a hard-sphere-like liquid does not have a homogeneous random structure, contrary to the common belief, but has a transient MRCO with hcp-like bond orientational order. The above result indicates that MRCO does not involve any density change and should not be regarded as prenuclei or small crystallites: MRCO is an intrinsic structural feature of a supercooled state, which is also confirmed from the presence of MRCO even in a system which never crystallizes (see figure 4). Furthermore, our result shows the important

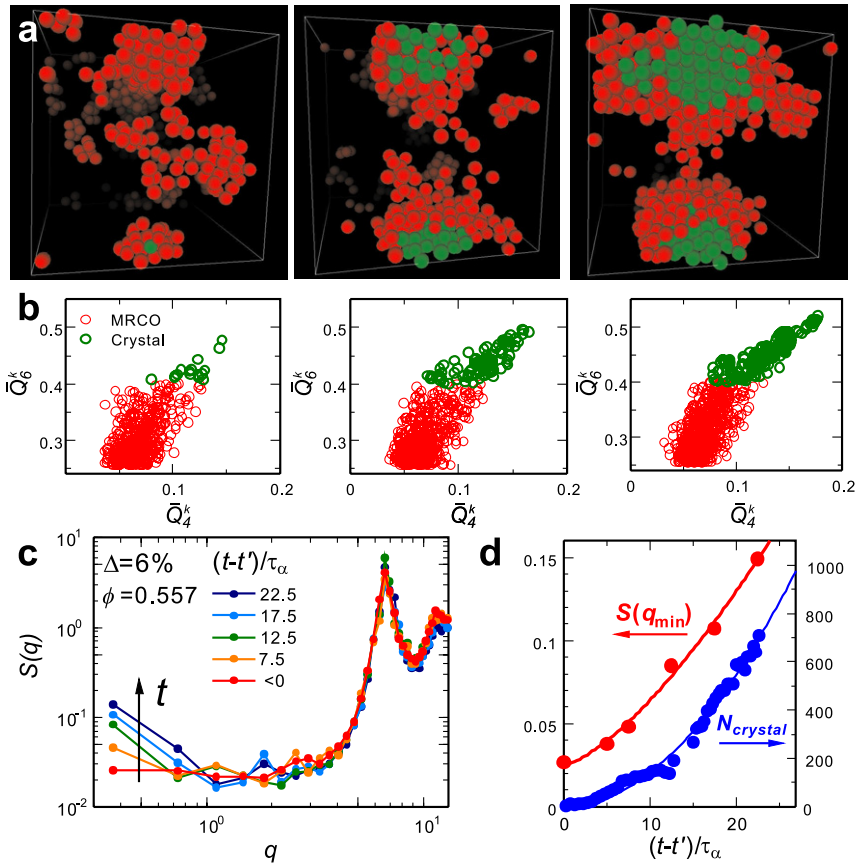

Figure 4. Birth of a crystal nucleus from MRCO. (a) The process of nucleation of a crystal at $\phi = 0.557$ and $\Delta = 6\%$. Particles with higher hcp BOO are coloured red, whereas those with higher fcc BOO are coloured green (see also (b)). We can see the birth of a crystal and its growth. $t = t'$, $t = t' + 5\tau_\alpha$, and $t = t' + 13\tau_\alpha$ from left to right. (b) Temporal change in the Q_4-Q_6 correlation map, corresponding to (a). (c) Temporal development of $S(q)$ during crystal nucleation and its growth. We can see the increase of $S(q)$ at low q for a system after crystal nucleation, indicating the density change upon crystallization. We emphasize that before crystal nucleation (for $(t - t')/\tau_\alpha < 0$) there is no excess scattering in the low q region in $S(q)$, which indicates the absence of density fluctuations associated with MRCO. (d) The temporal change in the number of particles in the crystal nucleus, which indicates the growth of the crystal nucleus, together with the temporal change in the scattering intensity $S(q_{\min})$ at the lowest wavenumber $q_{\min}$, which also indicates the growth of the nucleus and that the crystal nucleus has a higher density than the liquid.

role of MRCO in crystallization. A crystal nucleus is formed by thermal fluctuations preferentially inside regions of high MRCO because of the following reason: nucleation in a region of high MRCO leads to a small free-energy gain upon crystal ordering, but more importantly decreases the crystal–liquid interfacial energy drastically, which in total results in a large decrease in the nucleation barrier, i.e., the enhancement of the nucleation probability. We note that a crystal nucleus is almost perfectly embedded in a high MRCO region (coloured red), or perfectly wet to it. We stress that the roles of transient structural ordering (MRCO) in crystal nucleation has been completely overlooked so far. This novel scenario of enhancement of crystal nucleation may provide a clue as to why the nucleation frequency predicted by the existing theories is much lower (by many orders of magnitude in certain conditions) than that observed experimentally [44, 70–74]. Details will be reported elsewhere.

In relation to the above, it is worth mentioning a recent work by Pusey *et al* [50] on crystallization and glass formation in hard spheres. They proposed that the above-mentioned discrepancy between experiments and simulations reported by Auer and Frenkel [44] can largely be removed by taking into account the fact that the experimental volume fractions are (inappropriately) calculated assuming freezing to occur at $\phi = 0.494$, which is the value for a system of $\Delta = 0$ and should be replaced by 0.508 for a system of $\Delta = 5\%$ used in the experiments. This certainly reduces the discrepancy, but the ϕ-dependence of the nucleation frequency is still much steeper for simulations than for experiments. Furthermore, we recently found that the crystal nucleation frequency estimated by brute-force Brownian dynamics simulations is much faster than the prediction of Auer and Frenkel [44] even for a monodisperse colloidal system. So we believe that further studies are still necessary to resolve the discrepancy. Pusey *et al* [50, 69] also found an interesting novel kinetic route to crystals at high ϕ, which only requires a small rearrangement of the particle positions for crystallization to take place. We speculate that this new mode of crystallization may be related to the novel kinetic pathway to crystals found in this communication, i.e., preferential positional ordering in a region already having high hcp-like bond orientational order, since it should not require large rearrangement of particles.

3. Conclusions

In summary, we show a structural origin of dynamic heterogeneity for 3D polydisperse colloidal systems. In a supercooled liquid state, clusters of highly ordered particles emerge and they have a lifetime longer than the structural relaxation time τ_α (see figure S4, available at stacks.iop.org/JPhysCM/22/232102/mmedia). Particles belonging to clusters are less mobile, which explains dynamic heterogeneity. Furthermore, we show that the growth of MRCO is linked to slower dynamics. This growth of MRCO is more pronounced for a system with smaller Δ suffering from weaker frustration against crystallization. All these findings are common to 2D polydisperse colloidal systems [28], 2D driven granular liquids [29], and 2D frustrated spin liquids [27], suggesting some universality [61]. Since our system is a direct model of polydisperse colloidal liquids used in real experiments, similar behaviour is expected to be observed experimentally, which is actually supported by our preliminary experimental study by confocal microscopy. Another finding is that MRCO clusters have a hcp-like bond orientational order. This indicates that a supercooled liquid with hard-core repulsions has a tendency of crystal-like ordering but not icosahedral ordering. This seems not to be consistent with theories of glass transition, which assume the absence of any structure beyond a cage size and a tendency of icosahedral ordering, at least for polydisperse colloidal systems. The above finding supports a scenario [40] that frustration prevents global crystallization but a liquid still tends to be structured and attain transient medium-range structural order upon densification, which is a cause of dynamic heterogeneity and slow dynamics. At least in the present system, dynamic heterogeneity has a static thermodynamic origin rather than a dynamic one, contrary to its name. Here it may be worth noting a possible link of our MRCO with amorphous order [33], inherent structure [30, 38, 39], and defect density [32]. We argue that these structural signatures are all related to 'stress-bearing structures': MRCO characterizes a supercooled liquid state of a system suffering from weak geometrical frustration, whereas the others that suffering from strong frustration.

Our finding suggests that even a simple liquid has spatio-temporal hierarchy under supercooling: a supercooled liquid is 'inhomogeneous'. This may largely alter the classical picture of a supercooled liquid, which assumes that a liquid has a homogeneous structure-less random configuration. For example, we find that the existence of MRCO promotes crystal nucleation. We may say that 'homogeneous nucleation' can intrinsically have the nature of 'heterogeneous nucleation' in an exact sense. We emphasize that crystallization can in principle take place in a metastable supercooled state without any exception, or a supercooled liquid exhibiting slow dynamics always has a chance to be crystallized. Our findings suggest an intimate link between dynamic heterogeneity and crystal nucleation: glass transition may be frustration on the way to crystallization [27, 40]. Finally, we mention that the fact that a hard-sphere-like liquid tends to develop structural order upon densification casts some doubt on a popular proposition that an ideal glass has a random close packing structure, in line with [75]. Our study may shed new light on fundamental questions of whether an ideal glass transition exists or not [76] and what the structure of the ideal glass is if it exists.

Acknowledgments

This work was partially supported by a grant-in-aid from the Ministry of Education, Culture, Sports, Science and Technology, Japan.

References

[1] Anderson P W 1995 Through the glass lightly *Science* **267** 1615–6
[2] Angell C A 1995 Formation of glasses from liquids and biopolymers *Science* **267** 1924–35
[3] Debenedetti P G and Stillinger F H 1995 Supercooled liquids and the glass transition *Nature* **410** 259–67
[4] Ediger M D 2000 Spatially heterogeneous dynamics in supercooled liquids *Annu. Rev. Phys. Chem.* **51** 99–128
[5] Andersen H C 2005 Molecular dynamics studies of heterogeneous dynamics and dynamic crossover in supercooled atomic liquids *Proc. Natl Acad. Sci. USA* **102** 6686–91
[6] Sciortino F and Tartaglia P 2005 Glassy colloidal systems *Adv. Phys.* **54** 471–524
[7] Sillescu H 1999 Heterogeneity at the glass transition: a review *J. Non-Cryst. Solids* **243** 81–108
[8] Hurley M M and Harrowell P 1996 Non-Gaussian behavior and the dynamical complexity of particle motion in a dense two-dimensional liquid *J. Chem. Phys.* **105** 10521–6
[9] Yamamoto R and Onuki A 1997 Kinetic heterogeneities in a highly supercooled liquid *J. Phys. Soc. Japan* **66** 2545–8
[10] Yamamoto R and Onuki A 1998 Dynamics of highly supercooled liquids: heterogeneity, rheology, and diffusion *Phys. Rev.* E **58** 3515–29
[11] Kob W, Donati C, Plimpton S J, Poole P H and Glotzer S C 1997 Dynamical heterogeneities in a supercooled Lennard-Jones liquid *Phys. Rev. Lett.* **79** 2827–30
[12] Lačević N, Starr F W, Schroder T B and Glotzer S C 2003 Spatially heterogeneous dynamics investigated via a time-dependent four-point density correlation function *J. Chem. Phys.* **119** 7372–87
[13] Bennemann C, Donati C, Baschnagel J and Glotzer S C 1999 Growing range of correlated motion in a polymer melt on cooling towards the glass transition *Nature* **399** 246–9
[14] Kegel W K and van Blaaderen A 2000 Direct observation of dynamical heterogeneities in colloidal hard-sphere suspensions *Science* **287** 290–3
[15] Weeks E R, Crocker J C, Levitt A C, Schofield A and Weitz D A 2000 Three-dimensional direct imaging of structural relaxation near the colloidal glass transition *Science* **287** 627–31
[16] Berthier L, Biroli G, Bouchaud J P, Cipelletti L, El Masri D, L'Hôte D, Ladieu F and Pierno M 2005 Direct experimental evidence of a growing length scale accompanying the glass transition *Science* **310** 1797–800
[17] Poole P H, Glotzer S C, Coniglio A and Jan N 1997 Emergence of fast local dynamics on cooling toward the Ising spin glass transition *Phys. Rev. Lett.* **78** 3394–7
[18] Glotzer S C, Jan N, Lookman T, MacIsaac A B and Poole P H 1998 Dynamical heterogeneity in the Ising spin glass *Phys. Rev.* E **57** 7350–3
[19] Donati C, Douglas J F, Kob W, Plimpton S J, Poole P H and Glotzer S C 1998 Stringlike cooperative motion in a supercooled liquid *Phys. Rev. Lett.* **80** 2338–41

[20] Donati C, Glotzer S C, Poole P H, Kob W and Plimpton S J 1999 Spatial correlations of mobility and immobility in a glass-forming Lennard-Jones liquid *Phys. Rev.* E **60** 3107–19
[21] Dzugutov M, Simdyankin S I and Zetterling F H M 2002 Decoupling of diffusion from structural relaxation and spatial heterogeneity in a supercooled simple liquid *Phys. Rev. Lett.* **89** 195701
[22] Pusey P N and van Megen W 1986 Phase behaviour of concentrated suspensions of nearly hard colloidal spheres *Nature* **320** 340–2
[23] van Megen W and Underwood S M 1993 Glass transition in colloidal hard spheres: mode-coupling theory analysis *Phys. Rev. Lett.* **70** 2766–9
[24] Götze W and Sjögren L 1992 Relaxation processes in supercooled liquids *Rep. Prog. Phys.* **55** 241–376
[25] Brambilla G, El Masri D, Pierno M, Berthier L, Cipelletti L, Petekidis G and Schofield A B 2009 Probing the equilibrium dynamics of colloidal hard spheres above the mode-coupling glass transition *Phys. Rev. Lett.* **102** 085703
[26] Widmer-Cooper A and Harrowell P 2006 Predicting the long-time dynamic heterogeneity in a supercooled liquid on the basis of short-time heterogeneities *Phys. Rev. Lett.* **96** 185701
[27] Shintani H and Tanaka H 2006 Frustration on the way to crystallization in glass *Nat. Phys.* **2** 200–6
[28] Kawasaki T, Araki T and Tanaka H 2007 Correlation between dynamic heterogeneity and medium-range order in two-dimensional glass-forming liquids *Phys. Rev. Lett.* **99** 215701
[29] Watanabe K and Tanaka H 2008 Direct observation of medium-range crystalline order in granular liquids near the glass transition *Phys. Rev. Lett.* **100** 158002
[30] Matharoo G S, Gulam Razul M S and Poole P H 2006 Structural and dynamical heterogeneity in a glass-forming liquid *Phys. Rev.* E **74** 050502
[31] Hamanaka T and Onuki A 2007 Transitions among crystal, glass, and liquid in a binary mixture with changing particle-size ratio and temperature *Phys. Rev.* E **74** 011506
[32] Aharonov E, Bouchbinder E, Hentschel H G E, Ilyin V, Makedonska N, Procaccia I and Schupper N 2007 Direct identification of the glass transition: growing length scale and the onset of plasticity *Europhys. Lett.* **77** 56002
[33] Biroli G, Bouchaud J-P, Cavagna A, Grigera T S and Verrocchio P 2008 Thermodynamic signature of growing amorphous order in glass-forming liquids *Nat. Phys.* **4** 737–41
[34] Sausset F, Tarjus G and Viot P 2008 Tuning the fragility of a glass-forming liquid by curving space *Phys. Rev. Lett.* **101** 155701
[35] Sausset F and Tarjus G 2010 Growing static and dynamic length scales in a glass-forming liquid *Phys. Rev. Lett.* **104** 065701
[36] Yunker P, Zhang Z, Aptowicz K B and Yodh A G 2009 Irreversible rearrangements, correlated domains, and local structure in aging glasses *Phys. Rev. Lett.* **103** 115701
[37] Hedges L O, Jack R L, Garrahan J P and Chandler D 2009 Dynamic order–disorder in atomistic models of structural glass formers *Science* **323** 1309–13
[38] Stillinger F H and Weber T A 1982 Hidden structure in liquids *Phys. Rev.* A **25** 978–89
[39] Sciortino F, Kob W and Tartaglia P 1999 Inherent structure entropy of supercooled liquids *Phys. Rev. Lett.* **83** 3214–7
[40] Tanaka H 1999 Two-order-parameter description of liquids. i. A general model of glass transition covering its strong to fragile limit *J. Chem. Phys.* **111** 3163–74
[41] Tarjus G, Kivelson S A, Nussinov Z and Viot P 2008 The frustration-based approach of supercooled liquids and the glass transition: a review and critical assessment *J. Phys.: Condens. Matter* **17** R1143–82
[42] Weeks J D, Chandler D and Andersen H C 1971 Role of repulsive forces in determining the equilibrium structure of simple llquids *J. Chem. Phys.* **54** 5237–47
[43] Abraham S E, Bhattacharrya S M and Bagchi B 2008 Energy landscape, antiplasticization, and polydispersity induced crossover of heterogeneity in supercooled polydisperse liquids *Phys. Rev. Lett.* **100** 167801
[44] Auer S and Frenkel D 2001 Prediction of absolute crystal-nucleation rate in hard-sphere colloids *Nature* **409** 1020–3
[45] Dickinson E, Parker R and Lal M 1981 Polydispersity and the colloidal order–disorder transition *Chem. Phys. Lett.* **79** 578–82
[46] Henderson S I, Mortensen T C, Underwood S M and van Megen W 1996 Effect of particle size distribution on crystallisation and the glass transition of hard sphere colloids *Physica* A **223** 102–16
[47] Phan S E, Russel W B, Zhu J and Chaikin P M 1998 Effects of polydispersity on hard sphere crystals *J. Chem. Phys.* **108** 9789–95
[48] Williams S R, Snook I K and van Megen W 2001 Molecular dynamics study of the stability of the hard sphere glass *Phys. Rev.* E **64** 021506
[49] Fasolo M and Sollich P 2004 Fractionation effects in phase equilibria of polydisperse hard-sphere colloids *Phys. Rev.* E **70** 041410
[50] Pusey P N, Zaccarelli E, Valeriani C, Sanz E, Poon W C K and Cates M E 2009 Hard spheres: crystallization and glass formation *Phil. Trans. R. Soc.* A **367** 4993–5011
[51] Kofke D A and Bolhuis P G 1999 Freezing of polydisperse hard spheres *Phys. Rev.* E **59** 618–22
[52] Trusket T M, Torquato S, Sastry S, Debenedetti P G and Stillinger F H 1998 Structural precursor to freezing in the hard-disk and hard-sphere systems *Phys. Rev.* E **58** 3083–8
[53] Ebert F, Keim P and Maret G 2008 Local crystalline order in a 2d colloidal glass former *Eur. Phys. J.* E **28** 161–8
[54] Mattsson J, Wyss H M, Fernandez-Nieves A, Miyazaki K, Hu Z, Reichman D R and Weitz D A 2009 Soft colloids make strong glasses *Nature* **462** 83–6
[55] Steinhardt P J, Nelson D R and Ronchetti M 1983 Bond-orientational order in liquids and glasses *Phys. Rev.* B **28** 784–805
[56] ten Wolde P R, Ruiz-Montero M J and Frenkel D 1996 Numerical calculation of the rate of crystal nucleation in a Lennard-Jones system at moderate undercooling *J. Chem. Phys.* **104** 9932–47
[57] Lechner W and Dellago C 2008 Accurate determination of crystal structures based on averaged local bond order parameters *J. Chem. Phys.* **129** 114707
[58] Glaser M A and Clark N A 1993 Melting and liquid structure in two dimensions *Adv. Chem. Phys.* **83** 543–709
[59] Sachdev S and Nelson D R 1985 Order in metallic glasses and icosahedral crystals *Phys. Rev.* B **32** 4592–606
[60] Pronk S and Frenkel D 2003 Large difference in the elastic properties of fcc and hcp hard-sphere crystals *Phys. Rev. Lett.* **90** 255501
[61] Tanaka H, Kawasaki T, Shintani H and Watanabe K 2010 Critical-like behaviour of glass-forming liquids *Nat. Mater.* **9** 324–31
[62] Kirkpatrick T R, Thirumalai D and Wolynes P G 1989 Scaling concepts for the dynamics of viscous liquids near an ideal glassy state *Phys. Rev.* A **111** 1045–54
[63] Sethna J P, Shore J D and Huang M 1991 Scaling theory for the glass transition *Phys. Rev.* B **44** 4943–59
[64] Mittal J, Errington J R and Truskett T M 2006 Quantitative link between single-particle dynamics and static structure of supercooled liquids *J. Chem. Phys.* B **110** 18147–50
[65] Sharma R, Chakraborty S N and Chakravarty C 2006 Entropy, diffusivity, and structural order in liquids with waterlike anomalies *J. Chem. Phys.* **125** 204501

[66] Tarzia M and Moore M A 2007 Glass phenomenology from the connection to spin glasses *Phys. Rev.* E **75** 031502
[67] Elmatad Y S, Chandler D and Garrahan J P 2009 Corresponding states of structural glass formers *J. Phys. Chem.* B **113** 5563–7
[68] Saika-Voivod Ivan, Bowles R K and Poole P H 2009 Crystal nucleation in a supercooled liquid with glassy dynamics *Phys. Rev. Lett.* **103** 225701
[69] Zaccarelli E, Valeriani C, Sanz E, Poon W C K, Cates M E and Pusey P N 2009 Crystallization of hard-sphere glasses *Phys. Rev. Lett.* **103** 135704
[70] Palberg T 1999 Crystallization kinetics of repulsive colloidal spheres *J. Phys.: Condens. Matter* **11** R323–60
[71] Auer S and Frenkel D 2005 Numerical simulation of crystal nucleation in colloids *Adv. Polym. Sci.* **173** 149–208
[72] Sear R 2007 Nucleation: theory and applications to protein solutions and colloidal suspensions *J. Phys.: Condens. Matter* **19** 033101
[73] Gasser U 2009 Crystallization in three- and two-dimensional colloidal suspensions *J. Phys.: Condens. Matter* **21** 203101
[74] Harland J L, Henderson S I, Underwood S M and van Megen W 1995 Observation of accelerated nucleation in dense colloidal fluids of hard sphere particles *Phys. Rev. Lett.* **75** 3572–5
[75] Torquato S, Truskett T M and Debenedetti P G 2000 Is random close packing of spheres well defined? *Phys. Rev. Lett.* **84** 2064–7
[76] Donev A, Stillinger F H and Torquato S 2006 Do binary hard disks exhibit an ideal glass transition? *Phys. Rev. Lett.* **96** 225502